

Role of the $\Delta^*(1940)$ in the $\pi^+ p \rightarrow K^+ \Sigma^+(1385)$ and $pp \rightarrow nK^+ \Sigma^+(1385)$ reactions

Ju-Jun Xie,^{1,2,3,*} En Wang,^{4,†} and Bing-Song Zou^{3,‡}

¹*Institute of Modern Physics, Chinese Academy of Sciences, Lanzhou 730000, China*

²*Research Center for Hadron and CSR Physics, Institute of Modern Physics of CAS and Lanzhou University, Lanzhou 730000, China*

³*State Key Laboratory of Theoretical Physics, Institute of Theoretical Physics, Chinese Academy of Sciences, Beijing 100190, China*

⁴*Departamento de Física Teórica and IFIC, Centro Mixto Universidad de Valencia-CSIC, Institutos de Investigación de Paterna, Apartado 22085, E-46071 Valencia, Spain*

(Received 21 May 2014; revised manuscript received 17 July 2014; published 14 August 2014)

The $pp \rightarrow nK^+ \Sigma^+(1385)$ reaction is a very good isospin 3/2 filter for studying Δ^{++} resonance decaying to $K^+ \Sigma^+(1385)$. Within the effective Lagrangian method, we investigate the $\Sigma(1385)$ (spin parity $J^P = 3/2^+$) hadronic production in the $\pi^+ p \rightarrow K^+ \Sigma^+(1385)$ and $pp \rightarrow nK^+ \Sigma^+(1385)$ reactions. For the $\pi^+ p \rightarrow K^+ \Sigma^+(1385)$ reaction, in addition to the “background” contributions from t -channel K^{*0} exchange and u -channel $\Lambda(1115)$ and $\Sigma^0(1193)$ exchange, we also consider the contribution from the s -channel $\Delta^*(1940)$ resonance, which has significant coupling to the $K \Sigma(1385)$ channel. We show that the inclusion of the $\Delta^*(1940)$ resonance leads to a fairly good description of the low-energy experimental total cross section data of $\pi^+ p \rightarrow K^+ \Sigma^+(1385)$ reaction. Basing on the study of the $\pi^+ p \rightarrow K^+ \Sigma^+(1385)$ reaction and with the assumption that the excitation of $\Delta^*(1940)$ resonance dominates the $pp \rightarrow nK^+ \Sigma^+(1385)$ reaction, we calculate the total and differential cross sections of the $pp \rightarrow nK^+ \Sigma^+(1385)$ reaction. It is shown that the new experimental data support the important role played by the $\Delta^*(1940)$ resonance with a mass in the region of 1940 MeV and a width of around 200 MeV. We also demonstrate that the invariant mass distribution and the Dalitz plot provide direct information of the $\Sigma^+(1385)$ production, which can be tested by future experiments.

DOI: [10.1103/PhysRevC.90.025207](https://doi.org/10.1103/PhysRevC.90.025207)

PACS number(s): 13.75.-n, 14.20.Gk, 13.30.Eg

I. INTRODUCTION

Study of the spectrum of isospin 3/2 $\Delta^{++}(1232)$ excited states is one of the most important issues in hadronic physics and is attracting much attention because it is the most experimentally accessible system composed of three identical valence quarks. However, our knowledge on these resonances mainly comes from old πN experiments and is still very poor [1,2]. In the energy region around or above 2.0 GeV, there are still many theoretical predictions of “missing Δ^* states” within the constituent quark [3] or chiral unitary [4–7] approaches, which have so far not been observed. Searching for these “missing Δ^* states” from other production processes is necessary [8,9]. A possible new excellent source for studying these Δ^* resonances comprises the $\pi^+ p \rightarrow K^+ \Sigma^+(1385)$ and $pp \rightarrow nK^+ \Sigma^+(1385)$ reactions, which have a special advantage because there is no contribution from isospin 1/2 nucleon resonances because of the isospin and charge conservations. In addition, those reactions require the creation of an $\bar{s}s$ quark pair. Thus, a thorough and dedicated study of the strangeness production mechanism in those reactions has the potential to gain a deeper understanding of the interaction among strange hadrons and also the nature of the Δ^* resonances.

In analogy to the $\Delta(1232)$ as the first excited state of the nucleon, the $\Sigma(1385)$ is the first excited state of the $\Sigma(1193)$ hyperon and has a spin parity of $3/2^+$ and isospin 1. This

resonance is considered a standard quark triplet and cataloged in the baryon decuplet, but its vicinity to the $\Lambda(1405)$ state in the mass spectrum correlates the study and the understanding of the two resonances. Besides, a Σ state, $\Sigma(1380)$ (spin parity $J^P = 1/2^-$) with mass about 1380 MeV, was predicted in the framework of the diquark-diquark-antiquark picture [10–12]. This new state will have effects in the production of $\Sigma(1385)$ and then the analysis of the $\Sigma(1385)$ resonance suffers from the overlapping mass distributions and the common $\pi \Lambda(1115)$ decay mode.

There were pioneering measurements in the 1970s: The first $pp \rightarrow nK^+ \Sigma^+(1385)$ cross sections in the high-energy region, with beam momentum $p_{\text{lab}} = 6$ GeV, were reported in Ref. [13]. Recently, this reaction was examined at 3.5 GeV beam energy by HADES Collaboration [14]. The results of angular distributions of the $\Sigma^+(1385)$ in different reference frames show that there could be contribution from an intermediate Δ^* resonance via the decay of $\Delta^{++} \rightarrow K^+ \Sigma^+(1385)$. Thus, the study of the possible role played by Δ^* resonances in the available new data from the HADES Collaboration is timely and could shed light on the complicated dynamics that governs the spectrum of these Δ^* states.

The theoretical activity has also run in parallel. Thinking of the $pp \rightarrow nK^+ \Sigma^+(1385)$ reaction, the one-boson exchange model can be considered. By using this frame, several theoretical calculations by considering the π exchange diagrams [13], the π and K exchange diagrams [15], and the intermediate Δ^{++} excitation [16] exist for describing the old and high-energy data of Ref. [13]. These theoretical studies have traditionally been limited by the lack of knowledge on the $\Delta^* \Sigma(1385)K$ coupling strength and also the new experimental measurements from HADES [14].

* xiejujun@impcas.ac.cn

† En.Wang@ific.uv.es

‡ zoubs@itp.ac.cn

In this work, we study the $\pi^+p \rightarrow K^+\Sigma^+(1385)$ and $pp \rightarrow nK^+\Sigma^+(1385)$ reactions within the effective Lagrangian method by examining the important role of the Δ^* resonances in these reactions. For the $\pi^+p \rightarrow K^+\Sigma^+(1385)$ reaction, in addition to the “background” contributions from the t -channel K^{*0} exchange and u -channel $\Lambda(1115)$ and $\Sigma^0(1193)$ hyperon pole terms, we also study possible contributions from Δ^* resonances in the s -channel. Based on the results obtained from the $\pi^+p \rightarrow K^+\Sigma^+(1385)$ reaction, we tend to study the role of Δ^* resonances in the $pp \rightarrow nK^+\Sigma^+(1385)$ reaction with the assumption that the production mechanism is attributable to the π^+ -meson exchange with the aim of describing the new experimental data reported by HADES. Unfortunately, the information about the strong coupling of $\Delta^*K\Sigma(1385)$ is scarce [2]. Thus, it is necessary to rely on theoretical schemes, such as that of Refs. [17,18] based on a quark model (QM) for baryons. Among the possible Δ^* resonances, we have finally considered only the two-star D -wave $J^P = 3/2^- \Delta^*(1940)$, which is predicted to have visible contribution [18] to the $K\Sigma(1385)$ production. Indeed, in Refs. [19–22], the contribution from a Δ^* resonance with spin parity $3/2^-$ and mass around 2 GeV was studied in the $\gamma p \rightarrow K^+\Sigma^0(1385)$ reaction. They all found that this Δ^* resonance has a significant coupling to the $K\Sigma(1385)$ channel and plays an important role in the reaction of $\gamma p \rightarrow K^+\Sigma^0(1385)$.¹ Although the $\Delta^*(1940)$ resonance is listed in the Particle Data Group (PDG) book, the evidence of its existence is poor or only fair and further work is required to verify its existence and to know its properties; accordingly, its total decay width and branching ratios are not experimentally known, either. In this respect, the HADES measurements could be used to determine some properties of this resonance.

To end this Introduction, we would like to mention that in Refs. [19–22] the role played by another Δ^* resonance, $\Delta^*(2000)$ (spin parity $J^P = 5/2^+$), in the $\gamma p \rightarrow K^+\Sigma^0(1385)$ reaction has been also studied. In these works, it is shown that the $\Delta^*(2000)$ resonance has a dominant contribution. However, it is pointed out in Ref. [23] that the nominal mass of the $\Delta^*(2000)$ resonance does not correspond, in fact, to any experimental analysis but to an estimation based on the value of masses (~ 1740 and 2200 MeV) extracted from different data analysis [2]. From the results obtained in Ref. [23] we may conclude that the two distinctive resonances, $\Delta^*(\sim 1740)$ and $\Delta^*(\sim 2200)$, should be cataloged instead of $\Delta^*(2000)$. We thus do not consider the contribution from $\Delta^*(2000)$ resonance in the present work.

In the next section, we show the formalism and ingredients in our calculation, then numerical results and discussions are presented in Sec. III. A short summary is given in the last section.

¹In Refs. [20,21] the role played by the pentaquark state, $\Sigma^*(1380)$ (spin parity $J^P = 1/2^-$), is also studied. However, the knowledge on this state is very scarce. We thus leave the investigation of the role of this new state to a future study.

II. FORMALISM AND INGREDIENTS

The combination of an effective Lagrangian approach and the isobar model is an important theoretical tool in describing the various processes in the region of resonance produced. In this section, we introduce the theoretical formalism and ingredients to calculate the $\Sigma(1385)$ ($\equiv \Sigma^*$) hadronic production in $\pi^+p \rightarrow K^+\Sigma^+(1385)$ and $pp \rightarrow nK^+\Sigma^+(1385)$ reactions within the effective Lagrangian approach and isobar model.

Because we only consider the tree diagrams for the $\pi^+p \rightarrow K^+\Sigma^+(1385)$ and $pp \rightarrow nK^+\Sigma^+(1385)$ reactions, the total scattering amplitudes have not taken into account the unitary requirements, which may be important for extracting the parameters of the baryon resonances from the analysis of the experimental data [24,25], especially for those reactions involving many intermediate couple channels and three-particle final states [26,27]. However, we know that it is difficult to really apply the unitary constraints in the three-body cases, which need to include the complex loop diagrams [27–29], and the extracted rough parameters for the major resonances still provide useful information; hence, we will leave it to further studies. Nevertheless, our model used in the present work can give a reasonable description of the experimental data in the considered energy region. Meanwhile, our calculation offers some important clues for the mechanisms of the $\pi^+p \rightarrow K^+\Sigma^+(1385)$ and $pp \rightarrow nK^+\Sigma^+(1385)$ reactions and makes a first effort to study the role of the $\Delta^*(1940)$ resonance in the relevant reactions.

A. Feynman diagrams and effective interaction Lagrangian densities

The basic tree-level Feynman diagrams for the $\pi^+p \rightarrow K^+\Sigma^+(1385)$ and $pp \rightarrow nK^+\Sigma^+(1385)$ reactions are depicted in Figs. 1 and 2, respectively. For the $\pi^+p \rightarrow K^+\Sigma^+(1385)$ reaction, in addition to the “background” diagrams, such as t -channel K^{*0} exchange [Fig. 1(b)] and u -channel $\Lambda(1115)$ and $\Sigma^0(1193)$ exchange [Fig. 1(c)], we also consider the s -channel $\Delta^{++}(1940)$ ($\equiv \Delta^*$) resonance excitation process [Fig. 1(a)].

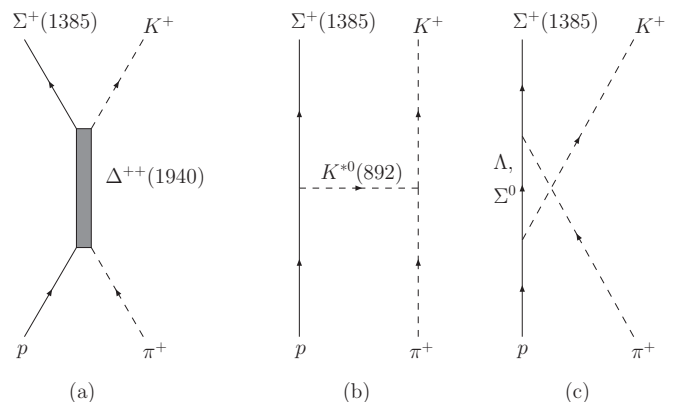


FIG. 1. Feynman diagrams for the $\pi^+p \rightarrow K^+\Sigma^+(1385)$ reaction. The contributions from s -channel $\Delta^{++}(1940)$ resonance, t -channel K^{*0} exchange, and u -channel $\Lambda(1115)$ and $\Sigma^0(1193)$ exchange are considered.

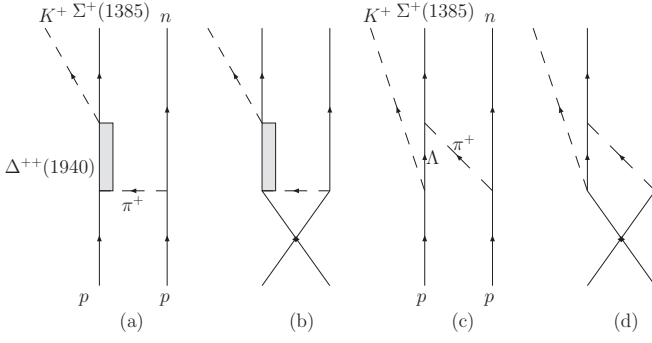


FIG. 2. Feynman diagrams for the $pp \rightarrow nK^+\Sigma^+(1385)$ reaction. Panels (a) and (c) show the direct processes, while (b) and (d) show the exchange processes.

In Fig. 2, we show the tree-level Feynman diagrams for the $pp \rightarrow nK^+\Sigma^+(1385)$ reaction. The diagram Figs. 2(a) and 2(c) show the direct processes, while Figs. 2(b) and 2(d) show the exchange processes. It is assumed that the production of the $K^+\Sigma^+(1385)$ passes mainly through the $\Delta^{++}(1940)$, which has a significant coupling to $K\Sigma(1385)$. In this case, the t -channel K^{*0} exchange and u -channel $\Sigma^0(1193)$ exchange processes are neglected because their contributions are small, which are discussed below.

For the $\pi^+p \rightarrow K^+\Sigma^+(1385)$ reaction, to compute the contributions of those terms shown in Fig. 1, we use the interaction Lagrangian densities as in Refs. [19,30,31],

$$\mathcal{L}_{\pi N\Delta^*} = \frac{g_{\pi N\Delta^*}}{m_\pi} \bar{\Delta}^{*\mu} \gamma_5 (\partial_\mu \vec{\tau} \cdot \vec{\pi}) N + \text{H.c.}, \quad (1)$$

$$\mathcal{L}_{K\Sigma^*\Delta^*} = \frac{g_1}{m_K} \bar{\Sigma}^{*\mu} \gamma_\alpha (\partial^\alpha K) \Delta^{*\mu} + \frac{ig_2}{m_K^2} \bar{\Sigma}^{*\mu} (\partial^\mu \partial_\nu K) \Delta^{*\nu} + \text{H.c.}, \quad (2)$$

for the s -channel $\Delta^*(1940)$ processes, and

$$\mathcal{L}_{K^*N\Sigma^*} = i \frac{g_{K^*N\Sigma^*}}{2m_N} \bar{N} \gamma^\nu \gamma_5 \Sigma^{*\mu} (\partial_\mu K_\nu^* - \partial_\nu K_\mu^*) + \text{H.c.}, \quad (3)$$

$$\mathcal{L}_{K^*K\pi} = g_{K^*K\pi} [\bar{K} (\partial^\mu \vec{\tau} \cdot \vec{\pi}) - (\partial^\mu \bar{K}) \vec{\tau} \cdot \vec{\pi}] K_\mu^* + \text{H.c.}, \quad (4)$$

for the t -channel K^{*0} exchange process, while

$$\mathcal{L}_{KN\Sigma/\Lambda} = -ig_{KN\Sigma/\Lambda} \bar{N} \gamma_5 K \Sigma/\Lambda + \text{H.c.}, \quad (5)$$

$$\mathcal{L}_{\Sigma^*\pi\Sigma/\Lambda} = \frac{g_{\Sigma^*\pi\Sigma/\Lambda}}{m_\pi} \bar{\Sigma}^{*\mu} (\partial_\mu \vec{\tau} \cdot \vec{\pi}) \Sigma/\Lambda + \text{H.c.}, \quad (6)$$

for the u -channel $\Sigma^0(1193)$ and $\Lambda(1115)$ exchange diagrams.

The above Lagrangian densities are also used to study the contributions of the terms shown in Fig. 2 for the $pp \rightarrow nK^+\Sigma^+(1385)$ reaction. In addition, we also need the Lagrangian density as follows for the πNN vertex:

$$\mathcal{L}_{\pi NN} = -ig_{\pi NN} \bar{N} \gamma_5 \vec{\tau} \cdot \vec{\pi} N. \quad (7)$$

B. Coupling constants and form factors

First, the coupling constant for the πNN vertex is taken to be $g_{\pi NN} = 13.45$, while the coupling constants $g_{KN\Sigma}$,

$g_{KN\Lambda}$, and $g_{K^*N\Sigma^*}$ are respectively taken as 2.69, -13.98 , and -5.48 , which are obtained from the SU(3) flavor symmetry. These values have also been used in previous works [9,19,31–33].

Second, the coupling constants, $g_{K^*K\pi}$, $g_{\Sigma^*\pi\Sigma}$, and $g_{\Sigma^*\pi\Lambda}$, are determined from the experimentally observed partial decay widths of $K^* \rightarrow K\pi$, $\Sigma(1385) \rightarrow \pi\Sigma$, and $\Sigma(1385) \rightarrow \pi\Lambda$, respectively. With the effective interaction Lagrangians described by Eqs. (4) and (6), the partial decay widths $\Gamma_{K^* \rightarrow K\pi}$ and $\Gamma_{\Sigma(1385) \rightarrow \pi\Sigma/\Lambda}$ can be easily calculated. The coupling constants are related to the partial decay widths as

$$\Gamma_{K^* \rightarrow K\pi} = \frac{g_{K^*K\pi}^2}{2\pi} \frac{|\vec{p}_\pi^{\text{c.m.}}|^3}{m_{K^*}^2}, \quad (8)$$

$$\Gamma_{\Sigma^* \rightarrow \pi\Sigma/\Lambda} = \frac{f_I g_{\Sigma^*\pi\Sigma/\Lambda}^2 |\vec{p}_{\Sigma/\Lambda}^{\text{c.m.}}|^3 (E_{\Sigma/\Lambda} + m_{\Sigma/\Lambda})}{12\pi m_\pi^2 M_{\Sigma^*}^2}, \quad (9)$$

with the isospin factor $f_I = 2$ for $\Sigma^* \rightarrow \pi\Sigma$ and $f_I = 1$ for $\Sigma^* \rightarrow \pi\Lambda$ and

$$E_{\Sigma/\Lambda} = \frac{M_{\Sigma^*}^2 + m_{\Sigma/\Lambda}^2 - m_\pi^2}{2M_{\Sigma^*}},$$

$$|\vec{p}_{\Sigma/\Lambda}^{\text{c.m.}}| = \sqrt{E_{\Sigma/\Lambda}^2 - m_{\Sigma/\Lambda}^2},$$

$$|\vec{p}_\pi^{\text{c.m.}}| = \frac{\sqrt{[m_{K^*}^2 - (m_K + m_\pi)^2][m_{K^*}^2 - (m_K - m_\pi)^2]}}{2m_{K^*}}.$$

With mass ($M_{\Sigma^*} = 1384.57$ MeV, $m_{K^*} = 893.1$ MeV), total decay width ($\Gamma_{\Sigma^*} = 37.13$ MeV, $\Gamma_{K^*} = 49.3$ MeV), and decay branching ratios of $\Sigma(1385)$ [$\text{Br}(\Sigma^* \rightarrow \pi\Sigma) = 0.117 \pm 0.015$, $\text{Br}(\Sigma^* \rightarrow \pi\Lambda) = 0.87 \pm 0.015$] and K^* [$\text{Br}(K^* \rightarrow K\pi) \sim 1$], we obtain these coupling constants as listed in Table I.

Finally, the strong coupling constants $g_{\pi N\Delta^*}$ and $g_{1,2}$ for the $\Delta^*(1940)\Sigma(1385)K$ vertex are free parameters, which will be determined by fitting to the experimental data on the total cross sections of the $\pi^+p \rightarrow K^+\Sigma^+(1385)$ reaction.

In evaluating the scattering amplitudes of the $\pi^+p \rightarrow K^+\Sigma^+(1385)$ and $pp \rightarrow nK^+\Sigma^+(1385)$ reactions, we need to include the form factors because the hadrons are not pointlike particles. We adopt here the common scheme used in many previous works,

$$f_i = \frac{\Lambda_i^4}{\Lambda_i^4 + (q_i^2 - M_i^2)^2}, \quad i = s, t, u, \quad (10)$$

$$\text{with } \begin{cases} q_s^2 = s, & q_t^2 = t, & q_u^2 = u, \\ M_s = M_{\Delta^*}, & M_t = m_{K^*}, \\ M_u = m_{\Sigma, \Lambda}, \end{cases} \quad (11)$$

²In principle, there are three terms for $K^*N\Sigma^*$ vertex as used in Ref. [19] [see Eq. (6) of that reference for more details]. However, there is no more information about this vertex, and it is found that the other two couplings give minor contributions to the $\gamma p \rightarrow K^+\Sigma^0(1385)$ reaction [19]. Thus, we ignore the contributions from the other two couplings.

TABLE I. Values of the coupling constants required for the estimation of the $\pi^+ p \rightarrow K^+ \Sigma^+(1385)$ and $pp \rightarrow nK^+ \Sigma^+(1385)$ reactions. These have been estimated from the decay branching ratios quoted in the PDG book [2], though it should be noted that these are for all final charged states.

Decay modes	Adopted branching ratios	g^a
$\Sigma^* \rightarrow \pi \Lambda$	0.87	1.26
$\Sigma^* \rightarrow \pi \Sigma$	0.12	0.69
$K^* \rightarrow K \pi$	1.00	3.24

^aIt should be stressed that the partial decay width determines only the square of the corresponding coupling constants, as shown in Eqs. (8) and (9); thus, their signs remain uncertain. Predictions from QM can be used to constrain these signs. Unfortunately, QM calculations for these vertices are still sparse. We thus choose a positive sign for these coupling constants.

where s , t , and u are the Lorentz-invariant Mandelstam variables. In the present calculation, $q_s = p_1 + p_2$, $q_t = p_1 - p_3$, and $q_u = p_4 - p_1$ are the 4-momentum of intermediate $\Delta^*(1940)$ resonance in the s -channel, exchanged $K^{*0}(892)$ meson in the t -channel, and exchanged $\Sigma^0(1193)$ and $\Lambda(1115)$ in the u -channel, respectively, while p_1 , p_2 , p_3 , and p_4 are the 4-momenta for π^+ , p , K^+ , and $\Sigma^+(1385)$, respectively. In principle, the cutoff Λ_s , Λ_t , and Λ_u are free parameters of the model, but in practice we constrain them to a common value between 0.6 and 1.2 GeV. By doing this, we can reduce the number of the free parameters.

C. Scattering amplitudes

The invariant scattering amplitudes that enter our model for calculation of the total cross sections for

$$\pi^+(p_1)p(p_2, s_p) \rightarrow K^+(p_3)\Sigma^+(1385)(p_4, s_{\Sigma^*}) \quad (12)$$

are defined as

$$-iT_i = \bar{u}_\mu(p_4, s_{\Sigma^*}) A_i^\mu u(p_2, s_p), \quad (13)$$

where u_μ and u are dimensionless Rarita-Schwinger and Dirac spinors, respectively, while s_{Σ^*} and s_p are the spin polarization variables for final $\Sigma^+(1385)$ and initial proton, respectively. To get the scattering amplitudes, we need also the propagators for $\Delta^*(1940)$, K^* meson, and Σ^0/Λ hyperon,

$$G_{K^*}^{\mu\nu}(q_t) = i \frac{-g^{\mu\nu} + q_t^\mu q_t^\nu / m_{K^*}^2}{t - m_{K^*}^2}, \quad (14)$$

$$G_{\Sigma^0/\Lambda}(q_u) = i \frac{\not{q}_u + m_{\Sigma^0/\Lambda}}{u - m_{\Sigma^0/\Lambda}^2}, \quad (15)$$

$$G_{\Delta^*}^{\mu\nu}(q_s) = i \frac{\not{q}_s + M_{\Delta^*}}{D} P^{\mu\nu}, \quad (16)$$

with

$$D = s - M_{\Delta^*}^2 + i M_{\Delta^*} \Gamma_{\Delta^*}, \quad (17)$$

$$P^{\mu\nu} = -g^{\mu\nu} + \frac{1}{3} \gamma^\mu \gamma^\nu + \frac{2}{3M_{\Delta^*}^2} q_s^\mu q_s^\nu + \frac{1}{3M_{\Delta^*}} (\gamma^\mu q_s^\nu - \gamma^\nu q_s^\mu), \quad (18)$$

where M_{Δ^*} and Γ_{Δ^*} are the mass and total decay width of the $\Delta^*(1940)$ resonance, respectively. Because M_{Δ^*} and Γ_{Δ^*} have large experimental uncertainties [2], we take them as free parameters and will fit them to the total cross sections of the $\pi^+ p \rightarrow K^+ \Sigma^+(1385)$ reaction.

Then, the reduced A_i^μ amplitudes in Eq. (13) can be easily obtained,

$$A_s^\mu = i \frac{g_{\pi N \Delta^*}}{m_\pi D} \left\{ \frac{g_1}{m_K} \not{p}_3 (\not{q}_s + M_{\Delta^*}) \left[p_1^\mu - \frac{1}{3} \gamma^\mu \not{p}_1 - \frac{1}{3M_{\Delta^*}} (\gamma^\mu q_s p_1 - q_s^\mu \not{p}_1) - \frac{2}{3M_{\Delta^*}^2} q_s^\mu q_s p_1 \right] - \frac{g_2}{m_K^2} (q_s + M_{\Delta^*}) p_3^\mu \left[p_1 p_3 - \frac{1}{3} \not{p}_3 \not{p}_1 - \frac{1}{3M_{\Delta^*}} (\not{p}_3 q_s p_1 - q_s p_3 \not{p}_1) - \frac{2}{3M_{\Delta^*}^2} q_s p_3 q_s p_1 \right] \right\} f_s, \quad (19)$$

$$A_t^\mu = \frac{\sqrt{2} g_{K^* K \pi} g_{K^* N \Sigma^*}}{m_N (t - m_{K^*}^2)} (\not{p}_3 p_1^\mu - \not{p}_1 p_3^\mu) f_t, \quad (20)$$

$$A_u^\mu = i \frac{g_{\Sigma^* \pi \Sigma^0/\Lambda} g_{K N \Sigma^0/\Lambda}}{m_\pi (u - m_{\Sigma^0/\Lambda}^2)} (q_u + m_{\Sigma^0/\Lambda}) \gamma_5 p_1^\mu f_u, \quad (21)$$

where the subindices s , t , and u stand for the s -channel $\Delta^*(1940)$, t -channel $K^{*0}(892)$ exchange, and u -channel $\Sigma^0(1193)$ and $\Lambda(1115)$ exchange, respectively. As we can see, in the tree-level approximation, only the products, such as $g_1 g_{\pi N \Delta^*}$ ($\equiv \tilde{g}_1$) and $g_2 g_{\pi N \Delta^*}$ ($\equiv \tilde{g}_2$) enter the invariant scattering amplitudes. Because the information on these couplings are scarce, they are also determined by fitting them to the low-energy experimental data on the total cross sections of the $\pi^+ p \rightarrow K^+ \Sigma^+(1385)$ reaction.

For the $pp \rightarrow nK^+ \Sigma^+(1385)$ reaction, the full invariant scattering amplitude in our calculation is composed of two parts corresponding to the s -channel $\Delta^*(1940)$ resonance and u -channel $\Lambda(1115)$ hyperon pole, which are produced by the π^+ -meson exchanges,

$$\mathcal{M} = \sum_{i=s,u} \mathcal{M}_i. \quad (22)$$

Each of the above amplitudes can be obtained straightforwardly with the effective couplings and following the Feynman rules. Here we give explicitly the amplitude \mathcal{M}_s ; for example,

$$\begin{aligned} \mathcal{M}_s &= \frac{\sqrt{2} g_{\pi N N} g_{\pi N \Delta^*}}{m_\pi} F_\pi^{NN}(k_\pi^2) F_\pi^{\Delta^* N}(k_\pi^2) F_s(q_{\Delta^*}^2) \\ &\times G_\pi(k_\pi^2) \bar{u}^\mu(p_4, s_4) \left(-\frac{g_1}{m_K} \not{p}_5 g_{\mu\rho} + \frac{g_2}{m_K^2} p_{5\mu} p_{5\rho} \right) \\ &\times G_{\Delta^*}^{\rho\sigma}(q_s) k_{\pi\sigma} \gamma_5 u(p_1, s_1) \bar{u}(p_3, s_3) \gamma_5 u(p_2, s_2) \\ &+ (\text{exchange term with } p_1 \leftrightarrow p_2), \end{aligned} \quad (23)$$

where $s_i (i = 1, 2, 3)$ and $p_i (i = 1, 2, 3)$ represent the spin projection and 4-momenta of the two initial protons and final neutron, respectively, while p_4 and p_5 are the 4-momenta of the final $\Sigma^+(1385)$ and K^+ meson, respectively, and s_4 stands for the spin projection of $\Sigma^+(1385)$. In Eq. (23), $k_\pi = p_2 - p_3$ and $q_{\Delta^*} = p_4 + p_5$ stand for the 4-momenta of the exchanged π^+ meson and intermediate $\Delta^*(1940)$ resonance, and $G_\pi(k_\pi^2)$ is the pion meson propagator,

$$G_\pi(k_\pi^2) = \frac{i}{k_\pi^2 - m_\pi^2}. \quad (24)$$

For the $pp \rightarrow nK^+\Sigma^+(1385)$ reaction, we need also the relevant off-shell form factors for πNN and $\pi N\Delta^*$ vertexes, which have been already included in the amplitude of Eq. (23), and we take them as

$$F_\pi^{NN}(k_\pi^2) = \frac{\Lambda_\pi^2 - m_\pi^2}{\Lambda_\pi^2 - k_\pi^2}, \quad (25)$$

$$F_\pi^{\Delta^*N}(k_\pi^2) = \frac{\Lambda_\pi^{*2} - m_\pi^2}{\Lambda_\pi^{*2} - k_\pi^2}, \quad (26)$$

with k_π the 4-momentum of the exchanged π meson. The cutoff parameters are taken as $\Lambda_\pi = \Lambda_\pi^* = 1.1$ GeV, with which the experimental data on the $pp \rightarrow nK^+\Sigma^+(1385)$ reaction can be reproduced.

D. Cross sections for the $\pi^+p \rightarrow K^+\Sigma^+(1385)$ reaction

The differential cross section for the $\pi^+p \rightarrow K^+\Sigma^+(1385)$ reaction at center of mass (c.m.) frame can be expressed as

$$\frac{d\sigma}{d\cos\theta} = \frac{1}{32\pi s} \frac{|\vec{p}_3^{\text{c.m.}}|}{|\vec{p}_1^{\text{c.m.}}|} \left(\frac{1}{2} \sum_{s_{\Sigma^*}, s_p} |T|^2 \right), \quad (27)$$

where θ denotes the angle of the outgoing K^+ relative to beam direction in the c.m. frame, while $\vec{p}_1^{\text{c.m.}}$ and $\vec{p}_3^{\text{c.m.}}$ are the 3-momentum of the initial π^+ and final K^+ mesons. The total invariant scattering amplitude T is given by

$$T = T_s + T_t + T_u. \quad (28)$$

From the amplitude, we can easily obtain the total cross sections of the $\pi^+p \rightarrow K^+\Sigma^+(1385)$ reaction as functions of the beam momentum p_{π^+} . By including all the contributions from the s -channel Δ^* resonance, t -channel $K^{*0}(892)$, and u -channel $\Sigma^0(1193)$ and $\Lambda(1115)$ processes at fixed cutoff parameters $\Lambda_s \neq \Lambda_t = \Lambda_u$, we perform a four-parameter ($M_{\Delta^*}, \Gamma_{\Delta^*}, \tilde{g}_1$, and \tilde{g}_2) χ^2 fit to the experimental data on total cross sections for the $\pi^+p \rightarrow K^+\Sigma^+(1385)$ reaction. There is a total of 11 data points below $p_{\pi^+} = 4$ GeV.

By constraining the value of the cutoff parameters Λ_s and $\Lambda_t = \Lambda_u$ from 0.6 to 1.2 GeV, we get the minimal χ^2/dof 0.8 with $\Lambda_t = \Lambda_u = 0.6$ GeV and $\Lambda_s = 0.9$ GeV, and the fitted parameters are $M_{\Delta^*} = 1940 \pm 24$ MeV, $\Gamma_{\Delta^*} = 172 \pm 94$ MeV, $\tilde{g}_1 = -0.36 \pm 0.19$, and $\tilde{g}_2 = 1.83 \pm 0.16$. The best fitting results for the total cross sections are shown in Fig. 3, comparing with the experimental data from Refs. [34–36]. The black solid line represents the full results,

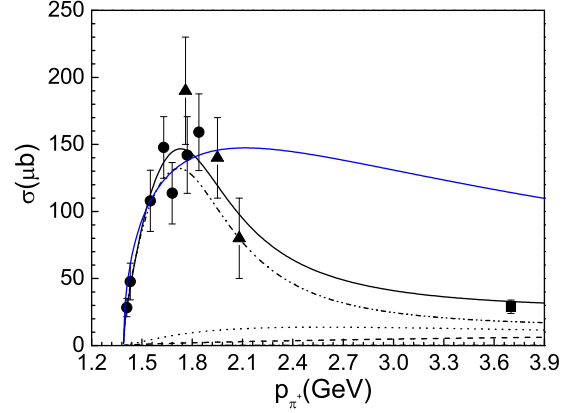


FIG. 3. (Color online) Total cross sections vs the beam momentum p_{π^+} for the $\pi^+p \rightarrow K^+\Sigma^+(1385)$ reaction. The experimental data are taken from Ref. [34] (dots), Ref. [35] (triangles), and Ref. [36] (square). The curves are the contributions from s -channel $\Delta^*(1940)$ (dash-dot-dotted), t -channel K^{*0} (dashed), u -channel $\Sigma^0(1193)$ (dash-dotted) and $\Lambda(1115)$ (dotted), and the total contributions of them (black-solid), respectively. The blue solid curve is obtained from the Stodolsky-Sakurai model, which is discussed below.

while the contributions from the s -channel $\Delta^{++*}(1940)$ resonance, t -channel $K^{*0}(892)$ exchange, and u -channel $\Lambda(1115)$ and $\Sigma^0(1193)$ terms are shown by the dash-dot-dotted, dashed, dotted, and dash-dotted lines, respectively. From Fig. 3, one can see that the description of the experimental data is quite good; especially, thanks to the contributions from the $\Delta^*(1940)$ resonance, the bump structure around $p_{\pi^+} = 1.8$ GeV can be described well. It is also shown that the s -channel $\Delta^*(1940)$ resonance gives the dominant contribution, while the t -channel and u -channel diagrams give the minor contributions.

In Fig. 4, the corresponding model predictions for the differential cross sections, $d\sigma/d\cos\theta$, of the $\pi^+p \rightarrow K^+\Sigma^+(1385)$ reaction are shown. Those results are obtained at $p_{\pi^+} = 1.42$ GeV [Fig. 4(a)], $p_{\pi^+} = 1.55$ GeV [Fig. 4(b)], $p_{\pi^+} = 1.62$ GeV [Fig. 4(c)], $p_{\pi^+} = 1.68$ GeV [Fig. 4(d)], $p_{\pi^+} = 1.77$ GeV [Fig. 4(e)], and $p_{\pi^+} = 1.84$ GeV [Fig. 4(f)], respectively. We also show the experimental data taken from Ref. [34] for comparison. One can see that by considering the dominant contributions from the $\Delta^*(1940)$, our model calculations can reasonably describe the angular distributions within the large experimental errors. However, at some energy points, such as $p_{\pi^+} = 1.55$ GeV [Fig. 4(b)], $p_{\pi^+} = 1.62$ GeV [Fig. 4(c)], and $p_{\pi^+} = 1.68$ GeV [Fig. 4(d)], our model calculations cannot well reproduce the experimental measurements.

It is pointed out that the Stodolsky-Sakurai model [37,38] with dominant contribution from t -channel K^* exchange fits those production angular distributions reasonably well at all beam momenta [34] (see more details in Fig. 4 of that reference). The predictions of this model are that the form of the differential cross sections for the $\pi^+p \rightarrow K^+\Sigma^+(1385)$ reaction is given by [34]

$$\frac{d\sigma}{d\cos\theta} \propto \frac{1 - \cos^2\theta}{(t - M_{K^*}^2)^2}, \quad (29)$$

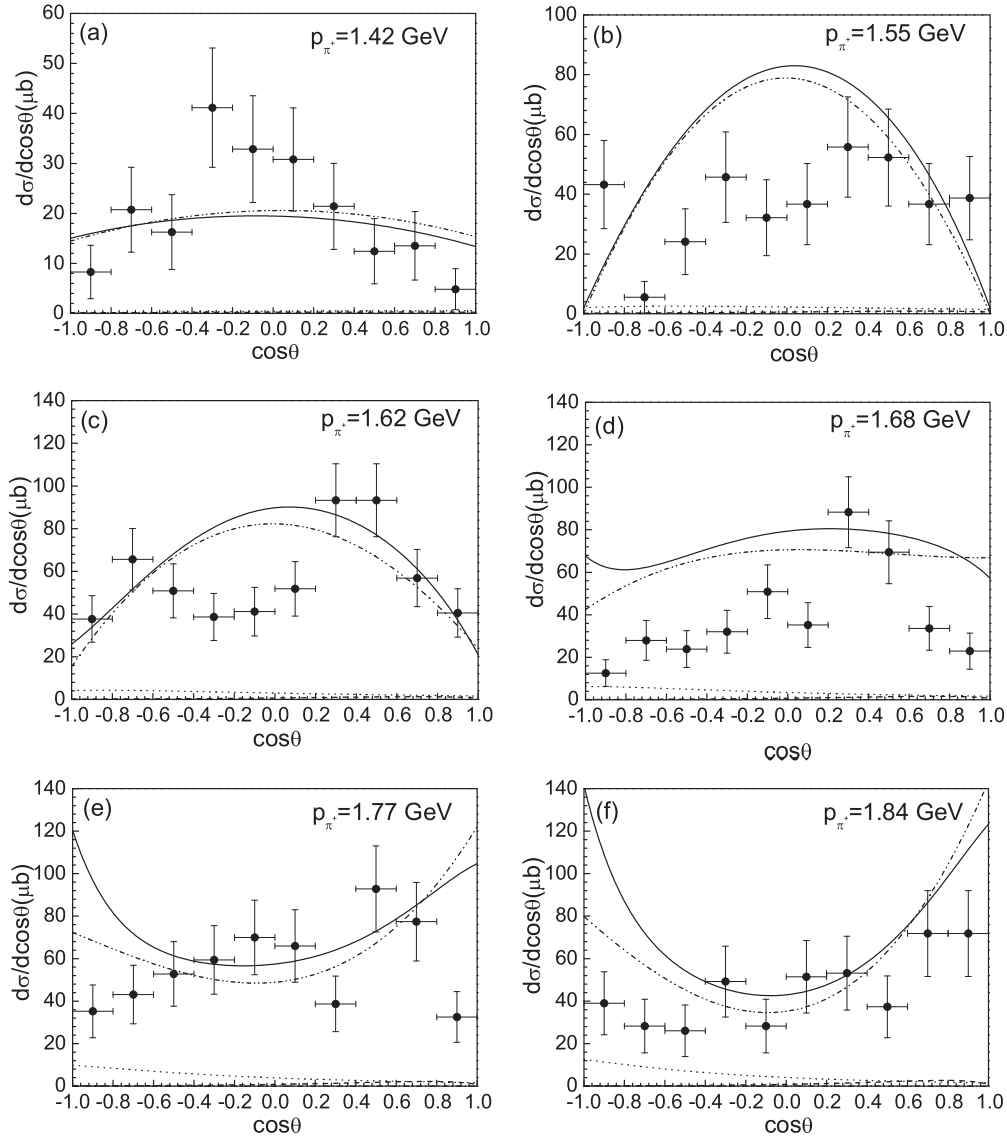


FIG. 4. Predictions of the differential cross sections, $d\sigma/d\cos\theta$, for the $\pi^+p \rightarrow K^+\Sigma^+(1385)$ reaction at different beam momenta. The experimental data are taken from Ref. [34]. The curves are the contributions from s -channel $\Delta^*(1940)$ (dash-dot-dotted), t -channel K^* (dashed), u -channel $\Sigma^0(1193)$ (dash-dotted) and $\Lambda(1115)$ (dotted), and the total contributions of them (solid), respectively.

from where we can obtain the total cross sections,³ as shown in Fig. 3 by the blue solid curve. One can see that the t -channel K^* exchange can reproduce well the experimental data from Ref. [34], but it cannot give the bump structure if we take those measurements of Refs. [35,36] into account as shown in Fig. 3. Thus, that the Stodolsky-Sakural model can reasonably describe the angular distribution at all momenta should not be surprising because it considered only the experimental data from Ref. [34], where the bump structure does not appear because of the narrow energy range of measurements of Ref. [34].

³We include also the phase-space factor, $|\vec{p}_3^{\text{c.m.}}|$, in our estimation. In this way, the total cross section is obtained from $\sigma = N \int_{-1}^1 \frac{1-\cos^2\theta}{(t-M_{K^*}^2)^2} |\vec{p}_3^{\text{c.m.}}| d\cos\theta$, with a normalization $N = 1.54 \text{ GeV}$.

However, we find that the experimental results of differential cross sections of Ref. [34] and the total cross sections data of Refs. [34–36] cannot be simultaneously fitted well, which is because the differential cross sections data with large uncertainties are inconsistent between different angles and energies; hence, those data points about the differential cross sections from Ref. [34] are not taken into account in our best fit.

E. Partial decay widths of the $\Delta^*(1940)$ resonance

With the Lagrangian densities of Eqs. (1) and (2), we can evaluate the $\Delta^*(1940)$ to $N\pi$ and $\Delta^*(1940)$ to $\Sigma(1385)K$ partial decay widths,

$$\Gamma_{\Delta^* \rightarrow N\pi} = \frac{g_{\pi N \Delta^*}^2}{12\pi} \frac{|\vec{p}_N^{\text{c.m.}}|^3}{m_\pi^2 M_{\Delta^*}} (E_N - m_N), \quad (30)$$

$$\begin{aligned} \Gamma_{\Delta^* \rightarrow \Sigma^* K} &= \frac{|\vec{p}_1^{\text{cm}}|(E_{\Sigma^*} + M_{\Sigma^*})}{36\pi M_{\Delta^*} M_{\Sigma^*}^2} \left\{ \frac{2g_2^2 M_{\Delta^*}^2}{m_K^4} |\vec{p}_1^{\text{cm}}|^4 + \frac{2g_1 g_2}{m_K^3} \right. \\ &\times M_{\Delta^*} (M_{\Delta^*} - M_{\Sigma^*}) (2E_{\Sigma^*} + M_{\Sigma^*}) |\vec{p}_1^{\text{cm}}|^2 + \frac{g_1^2}{m_K^2} \\ &\left. \times (M_{\Delta^*} - M_{\Sigma^*})^2 (2E_{\Sigma^*}^2 + 2E_{\Sigma^*} M_{\Sigma^*} + 5M_{\Sigma^*}^2) \right\}, \end{aligned} \quad (31)$$

where

$$E_N = \frac{M_{\Delta^*}^2 + m_N^2 - m_\pi^2}{2M_{\Delta^*}}, \quad (32)$$

$$|\vec{p}_N^{\text{c.m.}}| = \sqrt{E_N^2 - m_N^2}, \quad (33)$$

$$E_{\Sigma^*} = \frac{M_{\Delta^*}^2 + M_{\Sigma^*}^2 - m_K^2}{2M_{\Delta^*}}, \quad (34)$$

$$|\vec{p}_1^{\text{cm}}| = \sqrt{E_{\Sigma^*}^2 - M_{\Sigma^*}^2}. \quad (35)$$

With the values of M_{Δ^*} , Γ_{Δ^*} , \tilde{g}_1 , and \tilde{g}_2 obtained from the present fit, we get $\text{Br}(\Delta^* \rightarrow N\pi) \times \text{Br}(\Delta^* \rightarrow \Sigma^* K) = (0.52 \pm 0.13)\%$ with the error from the uncertainty of the fitted parameters.

Furthermore, the fitted results for the mass and total decay width of the $\Delta^*(1940)$ resonance are compatible with the previous analysis in Ref. [39],

$$M_{\Delta^*(1940)} = 1940 \pm 100 \text{ MeV}, \quad (36)$$

$$\Gamma_{\Delta^*(1940)} = 200 \pm 100 \text{ MeV}, \quad (37)$$

quoted in PDG [2]. Next, by using the branch ratio of $\text{Br}[\Delta^*(1940) \rightarrow N\pi]$ obtained in Ref. [39] and the total decay width of $\Gamma_{\Delta^*(1940)}$ from our present fit, we can determine the strong coupling constant, $g_{\pi N \Delta^*} = 0.35 \pm 0.12$ from the relation of Eq. (30). Then we can easily obtain the values of the strong $\Delta^*(1940)\Sigma(1385)K$ coupling constants g_1 and g_2 ,

$$g_1 = -1.04 \pm 0.38, \quad (38)$$

$$g_2 = 5.24 \pm 2.30. \quad (39)$$

Furthermore, the branch ratio $\text{Br}(\Delta^* \rightarrow \Sigma^* K)$ and partial decay width $\Gamma_{\Delta^* \rightarrow \Sigma^* K}$ are $(10.4 \pm 4.9)\%$ and $17.9 \pm 12.9 \text{ MeV}$, respectively. We find that the $\Sigma^* K$ decay mode of the $\Delta^*(1940)$ resonance could be larger than the $N\pi$ channel if one attributes the bump structure in the total cross sections of $\pi^+ p \rightarrow K^+ \Sigma^+(1385)$ reaction [34–36], to the effects produced by this resonance, as implicitly assumed in this work. This large coupling of the two-star D -wave $J^P = 3/2^- \Delta^*(1940)$ resonance to the $\Sigma^* K^+$ channel will confirm/get support from the QM results of Capstick and Roberts in Ref. [18], as mentioned above.

III. NUMERICAL RESULTS FOR THE $pp \rightarrow nK^+ \Sigma^+(1385)$ REACTION

With the formalism and ingredients given above, the calculations of the differential and total cross sections for

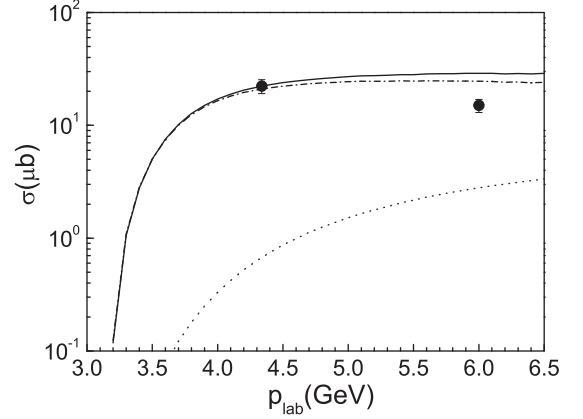


FIG. 5. Total cross sections vs beam energy p_{lab} of proton for the $pp \rightarrow nK^+ \Sigma^+(1385)$ reaction from the present calculation. The dotted and dash-dotted lines stand for contributions from $\Lambda(1115)$ pole and $\Delta^*(1940)$ resonance, respectively. Their total contribution are shown by the solid line. The experimental data are taken from Refs. [13,14].

$pp \rightarrow nK^+ \Sigma^+(1385)$ are straightforward,

$$\begin{aligned} d\sigma[pp \rightarrow nK^+ \Sigma^+(1385)] &= \frac{1}{4} \frac{m_p^2}{F} \sum_{s_1, s_2} \sum_{s_3, s_4} |\mathcal{M}|^2 \frac{m_n d^3 p_3}{E_3} \\ &\times \frac{m_{\Sigma^+(1385)} d^3 p_4}{E_4} \frac{d^3 p_5}{2E_5} \delta^4(p_1 + p_2 - p_3 - p_4 - p_5), \end{aligned} \quad (40)$$

with the flux factor

$$F = (2\pi)^5 \sqrt{(p_1 p_2)^2 - m_p^4}. \quad (41)$$

The total cross section versus the beam energy (p_{lab}) of the proton for the $pp \rightarrow nK^+ \Sigma^+(1385)$ reaction is calculated by using a Monte Carlo multiparticle phase space integration program. The results for beam energies p_{lab} from just above the production threshold 3.2 to 6.5 GeV are shown in Fig. 5. The dotted and dash-dotted lines stand for contributions from $\Lambda(1115)$ and $\Delta^*(1940)$ resonance, respectively. Their total contributions are shown by the solid line.⁴ From Fig. 5 we can see that the contribution from the $\Delta^*(1940)$ resonance is predominant in the whole considered energy region. For comparison, we also show the experimental data [13,14] in Fig. 5, from where we can see that our predictions for the total cross sections of $pp \rightarrow nK^+ \Sigma^+(1385)$ reaction are in agreement with the experimental measurements.

In addition to the total cross sections, we also compute the differential distributions for $pp \rightarrow nK^+ \Sigma^+(1385)$ reaction, namely, the angular distributions of all final-state particles in the overall center-of-mass frame (CMS), as well as distributions in both the Gottfried-Jackson and helicity frames

⁴Because the t -channel K^{*0} meson and u -channel $\Sigma^0(1193)$ exchange give very small contribution to the $\pi^+ p \rightarrow K^+ \Sigma^+(1385)$ reaction, especially for the invariant mass of $K\Sigma(1385)$ around 2 GeV, we ignore these contributions in the calculation for the $pp \rightarrow nK^+ \Sigma^+(1385)$ reaction.

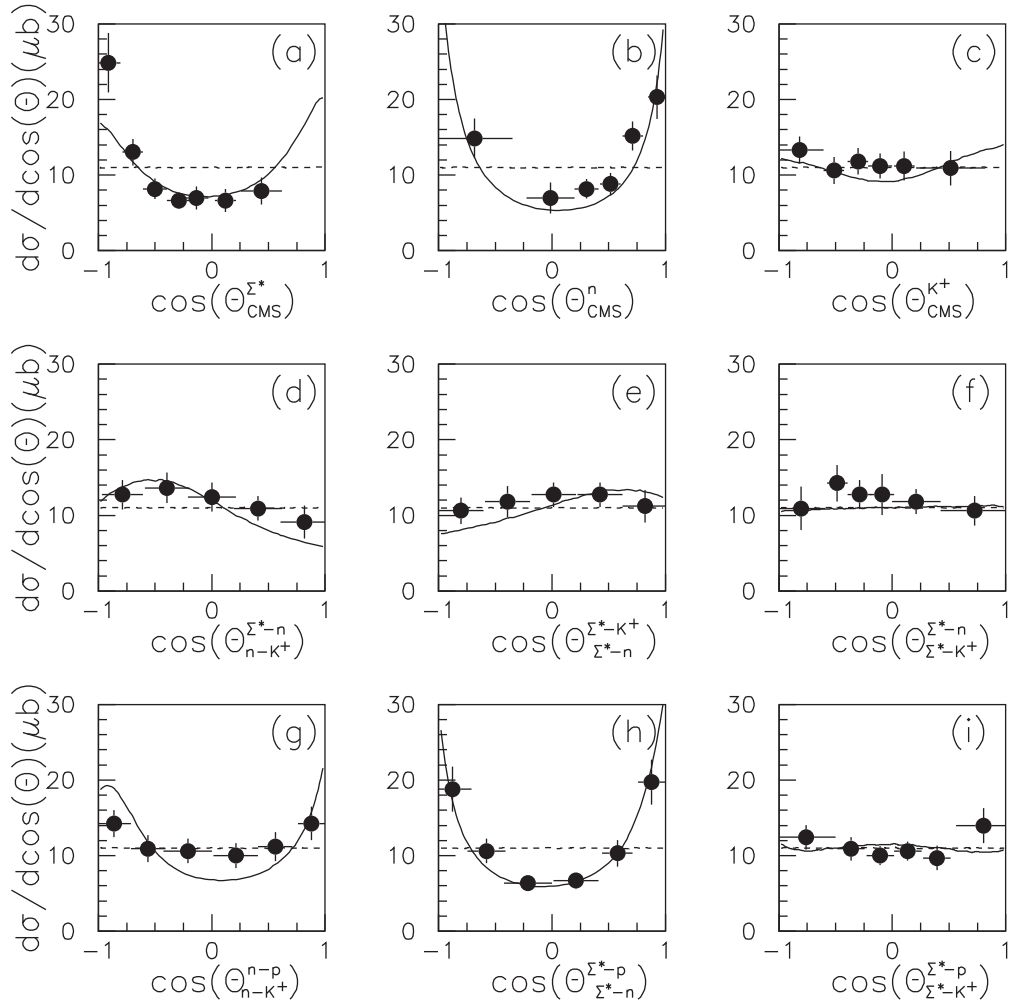


FIG. 6. Angular differential cross sections for the $pp \rightarrow nK^+\Sigma^+(1385)$ reaction in CMS [(a) $\Theta_{\text{CMS}}^{\Sigma^+}$, (b) Θ_{CMS}^n , (c) $\Theta_{\text{CMS}}^{K^+}$], helicity [(d) $\Theta_{n-K^+}^{\Sigma^+-n}$, (e) $\Theta_{\Sigma^+-K^+}^{\Sigma^+-n}$, (f) $\Theta_{\Sigma^+-K^+}^{\Sigma^+-n}$], and Gottfried-Jackson [(g) $\Theta_{n-K^+}^{n-p}$, (h) $\Theta_{\Sigma^+-n}^{\Sigma^+-p}$, (i) $\Theta_{\Sigma^+-K^+}^{\Sigma^+-p}$] reference frames. The dashed lines are pure phase-space distributions, while the solid lines are full results from our model. The experimental data are taken from Ref. [14].

as introduced in Refs. [14,40]. Like Dalitz plots, the helicity angle distributions provide insight into the three-body final state. While the information contained in the Gottfried-Jackson angle distributions is complementary to that of a Dalitz plot, as this angular distribution can give insight into the scattering process, especially concerning the involved partial waves.

The corresponding theoretical results are shown in Fig. 6 with the experimental data taken from Ref. [14], where the dashed lines are pure phase space distributions, while the solid lines are full results from our model. We can see that our theoretical results with the dominant contributions from the $\Delta^*(1940)$ resonance can describe the experimental data fairly well, and only the phase space is far from the data. The agreement of our model calculation with the experimental data in Fig. 6 indicates that the HADES data support the important role played by an odd-parity $3/2^- \Delta^*(1940)$ resonance with a mass in the region of 1940 MeV and a width of around 200 MeV.

In Figs. 6(a), 6(b), and 6(c), we show the $\Sigma^+(1385)$, neutron and K^+ angular distributions in the CMS, respectively. The anisotropy of the experimental distributions can be well

reproduced thanks to the contributions from the $\Delta^*(1940)$ resonance. The results obtained in the helicity frame with respect to the angle, Θ_{c-d}^{a-b} , which represents the angle between particles “a” and “b” in the “c” and “d” reference frame (see more details in Ref. [14]), are shown in Figs. 6(d), 6(e), and 6(f), while Figs. 6(g), 6(h), and 6(i) depict the distributions of the Gottfried-Jackson angles.

Furthermore, the corresponding momentum distribution⁵ of the $\Sigma^+(1385)$ and K^+ meson, the $K\Sigma(1385)$ invariant mass spectrum, and also the Dalitz Plot for the $pp \rightarrow nK^+\Sigma^+(1385)$ reaction at beam momentum $p_{\text{lab}} = 4.34$ GeV (corresponding to kinetic beam energy $T_p = 3.5$ GeV⁶), which is accessible for HADES Collaboration [14], are calculated and shown in Figs. 7(a), 7(b), 7(c), and 7(d), respectively. The dashed lines are pure phase-space distributions, while the

⁵It is noteworthy that our results are calculated in the reaction laboratory frame, in which the target proton is at rest.

⁶ $p_{\text{lab}} = \sqrt{E_{\text{lab}}^2 - m_p^2} = \sqrt{(T_p + m_p)^2 - m_p^2}$.

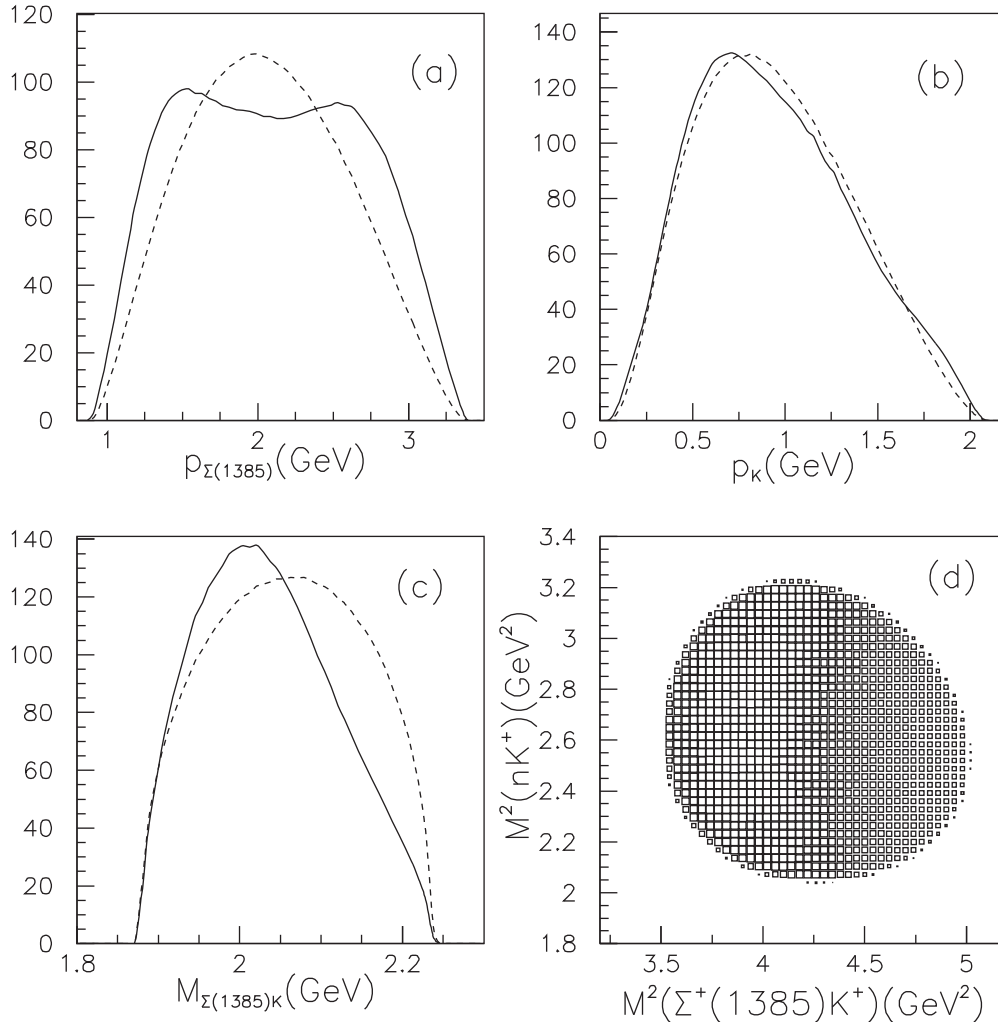


FIG. 7. Momentum distribution (arbitrary units), invariant mass spectrum (arbitrary units), and Dalitz plot for the $pp \rightarrow nK^+\Sigma^+(1385)$ reaction at beam energy $p_{\text{lab}} = 4.34$ GeV comparing with the phase-space distribution. The dashed lines are pure phase-space distributions, while the solid lines are full results from our model.

solid lines are full results from our model. From Fig. 7(c), we can see that at $p_{\text{lab}} = 4.34$ GeV our model results on the momentum distribution of the $\Sigma^+(1385)$ are much different with the phase space. However, there is a clear bump in the $K\Sigma(1385)$ invariant mass distribution, which is produced by including the contribution from the $\Delta^*(1940)$ resonance.

The momentum distribution, invariant mass spectra, and the Dalitz plots in Fig. 7 show direct information about the $pp \rightarrow nK^+\Sigma^+(1385)$ reaction mechanism and may be tested by future experiments.

In summary, owing to the important role played by the resonant contribution in the $pp \rightarrow nK^+\Sigma^+(1385)$ reaction, our model can describe the experimental data of the angle distributions well, which indicate that recent HADES data support the existence of this $\Delta^*(1940)$ resonance, and more accurate data for this reaction can be used to improve our knowledge on the $\Delta^*(1940)$ properties, which are, at present, poorly known. Our present calculation offers some important clues for the mechanisms of the $\pi^+p \rightarrow K^+\Sigma^+(1385)$ and $pp \rightarrow nK^+\Sigma^+(1385)$ reactions and makes a first effort to study the role of the $\Delta^*(1940)$ resonance in relevant reactions.

IV. SUMMARY

In this paper, the $\Sigma^+(1385)$ hadronic production in proton-proton and π^+p collisions are studied within the combination of the effective Lagrangian approach and the isobar model. For the $\pi^+p \rightarrow K^+\Sigma^+(1385)$ reaction, in addition to the “background” contributions from the t -channel $K^{*0}(892)$ exchange and u -channel $\Sigma^0(1193)$ and $\Lambda(1115)$ exchange, we also considered the contribution from the $\Delta^*(1940)$ resonance in the s -channel, which has significant coupling to $K\Sigma(1385)$ channel. We show that the inclusion of the $\Delta^*(1940)$ resonance leads to a fairly good description of the low-energy experimental total cross section data of the $\pi^+p \rightarrow K^+\Sigma^+(1385)$ reaction. The s -channel $\Delta^*(1940)$ resonance gives the dominant contribution, while the t -channel and u -channel diagrams give the minor contributions.

From χ^2 fit to the available experimental data for the $\pi^+p \rightarrow K^+\Sigma(1385)$ reaction, we get the mass and total decay width of $\Delta^*(1940)$, which are $M_{\Delta^*} = 1940 \pm 24$ MeV and $\Gamma_{\Delta^*} = 172 \pm 94$ MeV, respectively. With the value 0.35 ± 0.11 for the $\Delta^*(1940)N\pi$ coupling constant $g_{\pi N \Delta^*}$, which is

obtained with the branching ratio $\text{Br}[\Delta^*(1940) \rightarrow N\pi] = (5 \pm 2)\%$, we determine the strong couplings $g_{1,2}$ for the $\Delta^*(1940)K\Sigma(1385)$ vertex as $g_1 = -1.04 \pm 0.38$ and $g_2 = 5.24 \pm 2.30$. With these above values, we have calculated the partial decay width of $\Delta^*(1940) \rightarrow \Sigma(1385)K$, and we obtain $\Gamma_{\Delta^* \rightarrow \Sigma^*K} = 17.9 \pm 12.9$ MeV and $\text{Br}(\Delta^* \rightarrow \Sigma^*K) = (10.4 \pm 4.9)\%$. It is shown that the $\Delta^*(1940)$ resonance would have a large decay width into $\Sigma(1385)K$, which will be compatible with the findings of the QM approach of Ref. [18].

Based on the study of the $\pi^+p \rightarrow nK^+\Sigma^+(1385)$ reaction, we study the $pp \rightarrow nK^+\Sigma^+(1385)$ reaction with the assumption that the production mechanism is attributable to the π^+ -meson exchanges. We give our predictions about total cross sections for the $pp \rightarrow nK^+\Sigma^+(1385)$ reaction. We find that our theoretical results with the dominant contributions from the $\Delta^*(1940)$ resonance can describe fairly well the experimental data on both total cross sections and differential cross sections. Thus, the HADES data support the important role played by the $\Delta^*(1940)$ resonance with a mass in the region of 1940 MeV and a width of around 200 MeV. Furthermore, we also demonstrate that the invariant mass distribution and the Dalitz plot provide direct information of the $pp \rightarrow nK^+\Sigma^+(1385)$ reaction mechanisms and may be tested by the future experiments.

Finally, we would like to stress that the $pp \rightarrow nK^+\Sigma^+(1385)$ reaction is a new excellent source for studying

Δ^* resonances. Owing to the important role played by the $\Delta^*(1940)$ resonance in the $\pi^+p \rightarrow K^+\Sigma^+(1385)$ and $pp \rightarrow nK^+\Sigma^+(1385)$ reactions, accurate data for these reactions can be used to improve our knowledge on the $\Delta^*(1940)$ properties, which are, at present, poorly known.

ACKNOWLEDGMENTS

We would like to thank Juan Nieves, Bo-Chao Liu, and Xu Cao for useful discussions. This work is partly supported by DGI and FEDER funds, under Contracts No. FIS2011-28853-C02-01 and No. FIS2011-28853-C02-02, the Spanish Ingenio-Consolider 2010 Program CPAN (Grant No. CSD2007-00042), and Generalitat Valenciana under Contract No. PROMETEO/2009/0090 and by the National Natural Science Foundation of China under Grants No. 11105126, No. 11035006, No. 11121092, and No. 11261130311 (CRC110 by DFG and NSFC), the Chinese Academy of Sciences under Project No. KJCX2-EW-N01 and the Ministry of Science and Technology of China (Grant No. 2009CB825200). We acknowledge the support of the European Community-Research Infrastructure Integrating Activity ‘‘Study of Strongly Interacting Matter’’ (HadronPhysics3, Grant Agreement No. 283286) under the Seventh Framework Programme of EU.

-
- [1] E. Klempt and J. M. Richard, *Rev. Mod. Phys.* **82**, 1095 (2010).
 - [2] J. Beringer *et al.* (Particle Data Group), *Phys. Rev. D* **86**, 010001 (2012).
 - [3] S. Capstick and W. Robert, *Prog. Part. Nucl. Phys.* **45**, S241 (2000), and references therein.
 - [4] D. Gamermann, C. Garcia-Recio, J. Nieves, and L. L. Salcedo, *Phys. Rev. D* **84**, 056017 (2011).
 - [5] S. Sarkar, B.-X. Sun, E. Oset, and M. J. Vicente Vacas, *Eur. Phys. J. A* **44**, 431 (2010).
 - [6] E. Oset and A. Ramos, *Eur. Phys. J. A* **44**, 445 (2010).
 - [7] B.-X. Sun, H.-X. Chen, and E. Oset, *Eur. Phys. J. A* **47**, 127 (2011).
 - [8] J.-J. Xie and B.-S. Zou, *Phys. Lett. B* **649**, 405 (2007).
 - [9] M. Doring, C. Hanhart, F. Huang, S. Krewald, U.-G. Meissner, and D. Ronchen, *Nucl. Phys. A* **851**, 58 (2011).
 - [10] A. Zhang, Y. R. Liu, P. Z. Huang, W. Z. Deng, X. L. Chen, and S.-L. Zhu, *High Energy Phys. Nucl. Phys.* **29**, 250 (2005).
 - [11] J.-J. Wu, S. Dulat, and B. S. Zou, *Phys. Rev. D* **80**, 017503 (2009).
 - [12] J.-J. Wu, S. Dulat, and B. S. Zou, *Phys. Rev. C* **81**, 045210 (2010).
 - [13] S. Klein, W. Chinowsky, R. R. Kinsey, M. Mandelkern, J. Schultz, and T. H. Tan, *Phys. Rev. D* **1**, 3019 (1970).
 - [14] G. Agakishiev *et al.* (HADES Collaboration), *Phys. Rev. C* **85**, 035203 (2012).
 - [15] E. Ferrari, *Phys. Rev.* **175**, 2003 (1968).
 - [16] W. Chinowsky, R. R. Kinsey, S. L. Klein, M. Mandelkern, J. Schultz, F. Martin, M. L. Perl, and T. H. Tan, *Phys. Rev.* **165**, 1466 (1968).
 - [17] S. Capstick, *Phys. Rev. D* **46**, 2864 (1992).
 - [18] S. Capstick and W. Roberts, *Phys. Rev. D* **58**, 074011 (1998).
 - [19] Y. Oh, C. M. Ko, and K. Nakayama, *Phys. Rev. C* **77**, 045204 (2008).
 - [20] P. Gao, J.-J. Wu, and B. S. Zou, *Phys. Rev. C* **81**, 055203 (2010).
 - [21] Y.-H. Chen and B.-S. Zou, *Phys. Rev. C* **88**, 024304 (2013).
 - [22] J. He, *Phys. Rev. C* **89**, 055204 (2014).
 - [23] J.-J. Xie, A. Martinez Torres, E. Oset, and P. Gonzalez, *Phys. Rev. C* **83**, 055204 (2011).
 - [24] H. Kamano, B. Julia-Diaz, T.-S. H. Lee, A. Matsuyama, and T. Sato, *Phys. Rev. C* **80**, 065203 (2009).
 - [25] N. Suzuki, B. Julia-Diaz, H. Kamano, T.-S. H. Lee, A. Matsuyama, and T. Sato, *Phys. Rev. Lett.* **104**, 042302 (2010).
 - [26] H. Kamano, B. Julia-Diaz, T.-S. H. Lee, A. Matsuyama, and T. Sato, *Phys. Rev. C* **79**, 025206 (2009).
 - [27] H. Kamano, S. X. Nakamura, T. S. H. Lee, and T. Sato, *Phys. Rev. D* **84**, 114019 (2011).
 - [28] A. Martinez Torres, K. P. Khemchandani, U.-G. Meissner, and E. Oset, *Eur. Phys. J. A* **41**, 361 (2009).
 - [29] A. Martinez Torres, K. P. Khemchandani, and E. Oset, *Phys. Rev. C* **79**, 065207 (2009).
 - [30] B. S. Zou and F. Hussain, *Phys. Rev. C* **67**, 015204 (2003).
 - [31] S.-H. Kim, S.-I. Nam, A. Hosaka, and H.-C. Kim, *Phys. Rev. D* **88**, 054012 (2013).
 - [32] J.-J. Xie, B.-C. Liu, and C.-S. An, *Phys. Rev. C* **88**, 015203 (2013).
 - [33] J.-J. Xie and B.-C. Liu, *Phys. Rev. C* **87**, 045210 (2013).
 - [34] P. Hanson, G. E. Kalmus, and J. Louie, *Phys. Rev. D* **4**, 1296 (1971); see also <http://hepdata.cedar.ac.uk/view/ins74874>

- [35] S. Dagan, Z. Ming Ma, J. W. Chapman, L. R. Fortney, and E. C. Fowler, *Phys. Rev.* **161**, 1384 (1967).
- [36] W. R. Butler, D. G. Coyne, G. Goldhaber, J. Macnaughton, and G. H. Trilling, *Phys. Rev. D* **7**, 3177 (1973).
- [37] L. Stodolsky and J. J. Sakurai, *Phys. Rev. Lett.* **11**, 90 (1963).
- [38] L. Stodolsky, *Phys. Rev.* **134**, B1099 (1964).
- [39] R. E. Cutkosky, C. P. Forsyth, J. B. Babcock, R. L. Kelly, and R. E. Hendrick, in *Baryon 80: Proceedings of the 4th International Conference on Baryon Resonances, Toronto, Canada, July 14–16, 1980*, edited by N. Isgur (University of Toronto, Toronto, Canada, 1981), p. 19.
- [40] M. Abdel-Bary *et al.* (COSY-TOF Collaboration), *Eur. Phys. J. A* **46**, 27 (2010); **46**, 435 (2010).